Electronic Research Archive

ERA, 34(1): 657–675.
DOI: 10.3934/era.2026030
Received: 12 September 2025
Revised: 16 December 2025
Accepted: 25 December 2025
Published: 20 January 2026

http://www.aimspress.com/journal/era

Research article

Investigation of unsteady turbulent flow in the hydrodynamic entrance region of a circular cylindrical pipe

Arestak Sarukhanyan*, Garnik Vermishyan and Hovhannes Kelejyan

Department of Water Systems, Hydraulic Engineering and Hydropower, National University of Architecture and Construction of Armenia, 105 Teryan str., Yerevan, Armenia

* **Correspondence:** Email: asarukhanyan51@mail.ru.

Abstract: Regularities of viscous fluid flow in the hydrodynamic entrance region of a round pipe under turbulent unsteady flow conditions were studied, taking into account the tangential stresses that develop between the fluid layers. What distinguishes the proposed research is the method for generating tangential tensions between fluid layers, which impacts the accurate monitoring of the current hydrodynamic events. The study was based on the system of differential equations of viscous fluid flow, where viscous forces in turbulent flows were calculated using the Prandtl calculation method for stationary turbulent flows. Nevertheless, this formula could also be used in the case of unstable turbulent flows. This theory about the appearance of viscous forces in turbulent flows led to the creation of a mathematical model of the issue and the development of a method for its integration. Integration throughout the length of the inlet transition section led to the derivation of calculation formulas for the hydrodynamic properties of the current. These calculations showed the ongoing phenomena. In order to accurately design the transition sections of automatic hydrocontrolled equipment, it was crucial to understand the inlet transition section. Conclusions were drawn from the analysis of the results of computerized experimental research using the obtained analytical solutions. Scientific research and engineering applications may benefit from the study's findings.

Keywords: hydrodynamic entrance region; turbulent regime; velocity; unsteady flow

1. Introduction

A large number of studies of regularities of viscous fluid flow in the hydrodynamic entrance region of a round pipe under conditions of turbulent unsteady flow is stipulated with a need to increase the reliable set of design tools for automatic control of hydraulic systems. In applied fluid mechanics, unstable turbulent pressure flow is an issue that is extensively researched. The variety of unsteady pressure flow issues under investigation is large, notwithstanding the many and varied studies carried out, the outcomes obtained, and the use of contemporary computer techniques. This is explained by the fact that when developing methods for solving characteristic equations of unsteady pressure flows, it is often necessary to make assumptions that significantly limit the applicability of the obtained solution results. The results of solving the problem are often applicable to special cases of pressure flow, and new studies are needed to clarify or improve computational approaches. New research is required to explain or enhance computational methods, and the solutions to the problem are frequently relevant to specific instances of pressure flow. The study of hydrodynamic phenomena occurring in fluid-carrying channels is based on equations of motion of incompressible fluids, for the possible integration of which assumptions are made that limit their applicability. Very often, the proposed mathematical model of the problem reveals the picture of the ongoing physical phenomenon with acceptable accuracy. This will enable the proper construction of a specific hydrodynamic entry region, guaranteeing the structure's seamless, continuous operation. An applicable problem is the investigation of variations in the hydrodynamic characteristics of turbulent unstable flow at the entry of circular cylindrical pipes. To achieve this goal, a mathematical model of the problem was developed, based on the system of equations of one-dimensional unsteady flow of a viscous fluid. The friction forces developed between the fluid layers were calculated using the formula suggested by Prandtl for stationary turbulent flows, which is also acceptable for unsteady flows. The formulated boundary problem was integrated using the discontinuity method, as a result of which the patterns of changes in the hydrodynamic parameters of the flow were obtained in the studied domain. Based on the need of guaranteeing smooth operation, our findings revealed the primary challenges of accurately designing hydrodynamic entry regions of automatic systems.

A study was conducted to identify the patterns of change in the hydrodynamic parameters of a viscous fluid in the inlet region of a round cylindrical pipe during unsteady laminar flow [1]. However, the flow of a viscous fluid is mainly turbulent in nature; therefore, this study requires further development.

A comparative analysis of the results of analytical and numerical solutions of unsteady laminar flow at the inlet section of a round pipe was carried out [2]. Discrepancies between analytical and numerical solutions were revealed. Extensive experimental studies on unsteady laminar flows were carried out with comparative analytical and approximative analyses, and the intervals for using these solutions were determined [3]. A study of transient processes with a change in wave velocity along the length was conducted. Analytical solutions of laminar flow were obtained using the method of characteristics [4]. However, laminar flow is rarely encountered in practice. Additionally, viscous fluids usually move in a turbulent mode. In axisymmetric pipes, depending on the change in viscosity and pressure gradient, a method was developed for solving a boundary value problem to identify patterns of hydrodynamic parameters of laminar flow [5]. The general solution was obtained using the finite Hankel transform method. In [6], the unsteady laminar flow of a viscous incompressible fluid at the inlet section of a circular cylindrical pipe under general initial and boundary conditions was considered. In the area of sudden expansion of the cross-section of a cylindrical pipe, the patterns of

change in the hydrodynamic parameters of a viscous fluid under general boundary conditions were investigated [7]. The length of the transition section, which depends on the initial velocity distribution in the inlet section, was estimated. However, in [6,7,8], the research was conducted for laminar modes, which narrows the area of practical application of the results. Based on the research results, patterns of changes in speeds and pressure along the length of the transition section depending on time were revealed. Graphs of changes in the indicated physical quantities were constructed. A similar problem for stationary plane-parallel pressure flow was considered in [8].

The linear stability of steady flow in a round cylindrical pipe with a sudden increase in flow rate was considered. The characteristics of stability with stepwise changes in flow rate were investigated [9]. Based on the results of experimental studies, it was revealed that, depending on the Reynolds number, localized turbulent spots are formed behind the expansion [10]. An analysis of the mechanism of development of turbulent spots was given.

The numerical integration method was used to study the oscillatory plane-parallel pressure flow of a Newtonian fluid in the inlet region [11]. A calculation formula was obtained to determine the length of the hydrodynamic entrance region. In pressure systems, sections of sudden expansion of channels were often encountered. Based on the practical significance of the results of studying hydrodynamic processes at the site of sudden expansion of the channel, experimental studies of turbulent flow of fluid through channels of sudden expansion were conducted [12]. The characteristics of the recirculation zone flow in a sudden expansion pipe were obtained. Moreover, turbulence is the main cause of friction losses, and distortion of the velocity profile leads to the complete disappearance of turbulence. It has been shown that the return to laminar flow was achieved by an initial increase in turbulence intensity or a temporary increase in wall shear [13]. The flow characteristics in the recirculation zone in a pipe with a sudden expansion of 1:2 at a Reynolds number of 20,000 were analyzed.

The unsteady flow of an incompressible fluid in a round pipe with an arbitrary change in the kinematic viscosity coefficient over time was studied [14]. The results of the analytical solution were compared with the direct numerical solution of the momentum equation, and the difference was 1%. The presented analysis mainly relates to the study of hydrodynamic processes occurring at the entrance region of a circular cylindrical channel. Changes in the hydrodynamic parameters of the flow also occur at other transition points in the pipe: At the site of sudden widening of the section (D/d = 4), changes in the velocity and pressure of the viscous fluid in the axial direction were determined by numerical integration [15]. In [16], modeling the equations of flow of an incompressible fluid was carried out in areas of sudden changes in live shear, as a result of which the patterns of changes in the hydrodynamic parameters of the flow were revealed, and quantitative estimates were given [17]. Under conditions of symmetrical and asymmetrical expansions of the section, a dynamic change was realized. Changes in the hydrodynamic parameters of the flow also occur in other transition areas of the pipe. At the site of sudden widening of the section (D/d = 4), the changes in the velocity and pressure of the viscous fluid in the axial direction were determined by numerical integration [15] and numerical integration of differential equations [18]. Experimental studies were conducted to obtain quantitative estimates of the integration results [19]. The study was carried out for Newtonian and non-Newtonian fluids. Calculation formulas for the tangential stress components in turbulent flows were proposed in [20]. It has been shown that the turbulent tangential stress approaches faster in the flow direction than in the normal direction [21]. The reasons for this trend are explained by the formation of wall vortices. An analysis of the logarithmic profile of the velocity distribution in turbulent flow was performed in [22]. In the area of sudden widening of the section, researchers have measured the

changes in velocities in the direction of flow [23], which makes it possible to have an idea of the changes in velocities and draw conclusions. This is important for studying the properties of the flow. Moreover, using Prandtl's formula for the mixing path length in a smooth boundary layer, a smooth boundary turbulent flow simulation was performed [24], which resulted in the velocity distribution law in the boundary layer. However, these generalizations are not applicable to cylindrical or smooth pipes. In [25], the results of the transition period and turbulence were analyzed. However, despite the achievements, the results of studies identifying the emerging turbulent stress remain relevant. In [26], a method for controlling turbulent flow with the aim of reducing hydraulic resistance was developed. This was achieved using uniform and traveling wave oscillations of the wall, which reduces turbulent frictional resistance. Furthermore, numerical modeling of accelerated flow demonstrated that applied accelerations can significantly dampen oscillations [27]. In [28], a general method for the numerical solution of the problem of unsteady flow of a viscous incompressible fluid in flat channels of arbitrary shape was developed. The mathematical model of the flow was based on the two-dimensional Navier-Stokes equations and the Poisson equation for pressure, which were solved using the finite difference method.

The following tasks were solved to accomplish this goal:

1) Create a boundary value problem and devise a solution based on the Prandtl hypothesis regarding shear stresses of a turbulent flow,

2) Create graphs showing how axial velocities change over time and determine the requirements to identify out how long an axisymmetric pressure flow's inlet section should be during unsteady turbulent flow.

2. Materials and methods

2.1. Choosing a calculation scheme

The study of turbulent unsteady flow in the hydrodynamic entrance region of a round pipe is of important theoretical and applied interest (Figure 1). The analytical solution of the proposed problem was obtained based on the differential equations of non-deformable real fluid flow. The boundary conditions of the problem were defined in accordance with the conditions of flow.

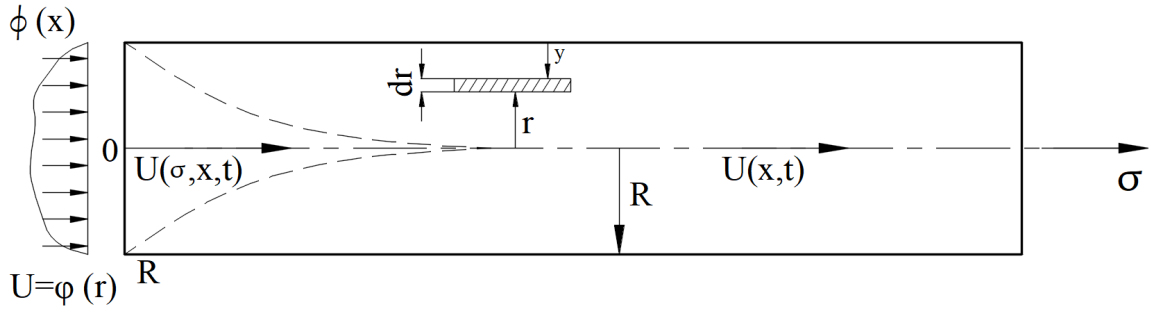

Figure 1. Hydrodynamic entrance region diagram for relevant calculations.

It is of significant theoretical and practical importance to investigate turbulent unsteady flow at

the hydrodynamic entry area of a circular pipe (Figure 1). The differential equations of non-deformable real fluid flow served as the foundation for the analytical solution of the suggested issue. The problem's boundary conditions were established in compliance with the flow conditions.

In the case of a linear approximation, the system of differential equations for the unsteady flow of a viscous fluid [29,30] will be:

$$\frac{\partial u}{\partial t}+U_{\circ}\frac{\partial u}{\partial z}=-\frac{1}{\rho}\cdot\frac{\partial p}{\partial z}+\frac{1}{\rho\cdot r}\left(r\cdot\frac{\partial \tau}{\partial r}+\tau\right), \tag{1}$$

$$\frac{\partial p}{\partial r}=0\ , \tag{2}$$

$$\frac{\partial u}{\partial z}+\frac{1}{r}\cdot\frac{\partial}{\partial r}\left(r\cdot V\right)=0\ , \tag{3}$$

$$U_{\circ}=\frac{2}{R^2\cdot\Delta T}\int_0^R\int_0^{\Delta T} r\cdot u\cdot dr\cdot dt\ , \tag{4}$$

where z axis is, and its origin is at the center of the initial cut. u and V are the velocity components in z and r axes, respectively. Eqs (1)–(3) are approximated differential equations for the axisymmetric flow of a viscous fluid in a circular pipe, whereas Eq (4) represents the cross-sectional average velocity.

$$u=u(z,r,t),\ \ V=V(z,r,t), \tag{5}$$

$$p=p(z,t) \tag{6}$$

where p is the pressure along the z-axis, which depends on the z and t coordinates, ρ is the density of the fluid, and τ is the shear stress developing between the layers.

For the differential equations of flow, the initial and boundary conditions are given, which, for the given problem, will be:

$$u=0,\ \ \text{at}\ \ r=R, \tag{7}$$

$$u=\Psi(r),\ \ V=0,\ \ \text{at}\, z=0,\quad 0\le r<R,\ \ t=0, \tag{8}$$

$$\frac{\partial U}{\partial z}\to 0,\ \ V=0,\ \ u\to u',\quad \text{at}\ \ z\to\infty, \tag{9}$$

where $u'=u'(r,t)$ is the solution to the equation of unsteady, axisymmetric one-dimensional flow. The axisymmetric unsteady equation has the following form [29]:

$$\frac{\partial u'}{\partial t} = -\frac{1}{\rho}\frac{\partial P}{\partial z} + \frac{\tau}{\rho}\left(\frac{\partial^2 u'}{\partial r^2} + \frac{1}{r}\frac{\partial u'}{\partial r}\right) \tag{10}$$

The shear stresses arising between layers due to active mixing of fluid particles in a turbulent flow are determined by the Prandtl formula [29]

$$\tau = \rho \ell^2 \left(\frac{du}{dy}\right)^2, \tag{11}$$

where ℓ is the length of the fluid particles mixing path,

$$\ell = \varepsilon . y, \tag{12}$$

where y is the distance of the layer from the fixed wall, as shown in Figure 1, and ε is the coefficient of proportionality, which is equal to 0.4 [29].
By inserting the calculation formula for turbulent shear stresses into Eq (1), we get

$$\frac{\partial u(z,y,t)}{\partial t} + U_0 \frac{\partial u(z,y,t)}{\partial z} = -\frac{1}{\rho}\frac{\partial p(z,t)}{\partial z} - \frac{1}{\rho}\left(\frac{\partial \tau(y,t)}{\partial y} - \frac{\tau(y,t)}{R-y}\right). \tag{13}$$

Let us introduce some dimensionless variables:

$$U(\sigma,x,t) = \frac{u(\sigma,x,t)}{U_0(\sigma,t)}, \frac{y}{R} = x, \frac{P}{P_0} = p,\ \sigma = \frac{z}{R}, -\frac{p_0}{\rho R U_0}\frac{\partial p(\sigma,t)}{\partial \sigma} = F(\sigma,t), \tau = \rho \varepsilon^2 U_0^2 \left(x\frac{dU}{dx}\right)^2. \tag{14}$$

The differential equation of the flow with dimensionless variables (13) will take the following form:

$$\frac{\partial U(\sigma,x,t)}{\partial t} + U_0 \frac{\partial U(\sigma,x,t)}{R\partial \sigma} = -\frac{P_0}{\rho R U_0}\frac{\partial p(\sigma,t)}{\partial \sigma} - \beta\left[\frac{\partial}{\partial x}\left(x\frac{\partial U(\sigma,x,t)}{\partial x}\right)^2 - \frac{x^2}{1-x}\left(\frac{\partial U(\sigma,x,t)}{\partial x}\right)^2\right], \tag{15}$$

where $\beta = \dfrac{\varepsilon^2 U_0}{R}$.

2.2. Statement of the problem and formulation of the system of differential

The initial conditions for the integration of the differential equation (15) will be

$$U = 0, \quad \text{at} \quad x = 0,\ \sigma > 0, \tag{16}$$

$$U(0,x,t) = \phi(x), \text{ at } \sigma = 0,\ 0 \le x \le 1, \qquad \sigma = 0,\ x = 1. \tag{17}$$

The solution to Eq (15) is presented in the form of a sum [31]

$$U(\sigma,x,t)=U_1(\sigma,x)+U_2(\sigma,x,t) \tag{18}$$

where the function $U_1(\sigma,x)$ is the solution of the homogeneous Eq (19)

$$\frac{\partial U_1(\sigma,x)}{\partial\sigma}=-\varepsilon^2\left[\frac{\partial}{\partial x}\left(x\frac{\partial U_1(\sigma,x)}{\partial x}\right)^2-\frac{x^2}{1-x}\left(\frac{\partial U_1(\sigma,x)}{\partial x}\right)^2\right] \tag{19}$$

and the function $U_2(\sigma,x,t)$ is the solution to the inhomogeneous differential equation (20)

$$\frac{\partial U_2(\sigma,x,t)}{\partial t}+\frac{U_0}{R}\frac{\partial U_2(\sigma,x,t)}{\partial\sigma}=-\frac{P_0}{\rho RU_0}\frac{\partial p(\sigma,t)}{\partial\sigma}-\beta\left[\frac{\partial}{\partial x}\left(x\frac{\partial U_2(\sigma,x,t)}{\partial x}\right)^2-\frac{x^2}{1-x}\left(\frac{\partial U_2(\sigma,x,t)}{\partial x}\right)^2\right] \tag{20}$$

The solution to Eq (19) will be

$$U_1(\sigma,x)=V(x)\cdot\exp\left(-\varepsilon^2\sigma\right), \tag{21}$$

then, we have

$$V(x)=\exp\left(-\varepsilon^2\sigma\right)\left[\frac{d}{dx}\left(x\frac{dV(x)}{dx}\right)^2-\frac{x^2}{1-x}\left(\frac{dV(x)}{dx}\right)^2\right] \tag{22}$$

The last equation is presented in the form of a system:

$$\begin{cases}W(x)=x\dfrac{dV(x)}{dx},\\ V(x)=2aW(x)\dfrac{dW(x)}{dx}-a\dfrac{W^2(x)}{1-x}\end{cases} \tag{23}$$

where $a=\exp\left(-\varepsilon^2\sigma_0\right)$.

The solution of the above system according to [31] will be:

$$W(x)=C_1+\int_1^x\xi V'(\varsigma)d\varsigma \tag{24}$$

By inserting this value of $W(x)$ into the Eq (23) system, we obtain the following equation for determining the function $V(x)$

$$V'(x)+xV''(x)=xV'(x) \tag{25}$$

The solution of Eq (25) is

$$V(x)=C_1\int_{0.01}^{x}\frac{e^{\xi}}{\xi}d\xi+C_2 \tag{26}$$

Considering the boundary condition of the problem $V(0)=0$, we get $C_2=0$. Therefore,

$$V(x)=C_1\int_{0.01}^{x}\frac{e^{\xi}}{\xi}d\xi \tag{27}$$

The solution to Eq (20) looks like this:

$$U_2(\sigma,x,t)=\varphi(\sigma,t)V(x), \tag{28}$$

and hence, we get

$$V(x)\left[\frac{\partial\varphi(\sigma,t)}{\partial t}+\frac{U_0}{R}\frac{\partial\varphi(\sigma,t)}{\partial\sigma}\right]=-\frac{P_0}{\rho RU_0}\frac{\partial p(\sigma,t)}{\partial\sigma}-\beta\varphi^2(\sigma,t)\left[\frac{d}{dx}(xV')^2-\frac{(xV')^2}{1-x}\right]. \tag{29}$$

Taking into account Eq (22), the last equation will take the following form:

$$V(x)\left[\frac{\partial\varphi(\sigma,t)}{\partial t}+\frac{U_0}{R}\frac{\partial\varphi(\sigma,t)}{\partial\sigma}+\frac{\beta}{a}\varphi^2(\sigma,t)\right]=-F(\sigma,t), \tag{30}$$

where

$$F(\sigma,t)=\frac{P_0}{\rho RU_0}\frac{\partial p(\sigma,t)}{\partial\sigma}. \tag{31}$$

Integrating Eq (28) over the interval [0.01, 1], we get:

$$\frac{\partial\varphi(\sigma,t)}{\partial t}+\frac{U_0}{R}\frac{\partial\varphi(\sigma,t)}{\partial\sigma}+\frac{\beta}{a}\varphi^2(\sigma,t)+\gamma=0, \tag{32}$$

here

$$\gamma=-\frac{0.99f(\sigma,t)}{b},\quad b=\int_{0.01}^{1}V(x)dx \tag{33}$$

We will get the solution of Eq (32) in the following form:

$$\varphi(\sigma,t)=\exp\left(-\varepsilon^2\sigma\right)\psi(t). \tag{34}$$

After this assignment, Eq (32) will be transformed into the following form:

$$\exp\left(-\varepsilon^2\sigma\right)\frac{\partial\psi(t)}{\partial t}-\frac{\varepsilon^2U_0}{R}\exp\left(-\varepsilon^2\sigma\right)\psi(t)+\frac{\beta}{a}\exp\left(-2\varepsilon^2\sigma\right)\psi^2(t)+\gamma=0. \tag{35}$$

Taking into account that $\exp\left(-\varepsilon^2\sigma\right)=1$ when σ=0, we get:

$$\frac{\partial\psi(t)}{\partial t}-\beta\psi(t)+\frac{\beta}{a}\psi^2(t)+\gamma=0. \tag{36}$$

The resulting equation has real roots when $a=\exp\left(-\varepsilon^2\sigma\right)=1$. In this case, we have:–

$$\psi(t)=\frac{1}{2}\left\{1+\sqrt{\frac{4\gamma-\beta}{\beta}}Tan\left[\frac{\sqrt{\beta}}{2}\left(\sqrt{4\gamma-\beta}C_0-\sqrt{4\gamma-\beta}t\right)\right]\right\}. \tag{37}$$

By substituting the values of the functions $\varphi(\sigma,t)$ and $\psi(t)$ into Eq (28), the function U_2 (σ, x, t) is determined:

$$U_2(\sigma,x,t)=\frac{1}{2}\exp\left(-\varepsilon^2\sigma\right)\left\{1+\sqrt{\frac{4\gamma-\beta}{\beta}}Tan\left[\frac{\sqrt{\beta}}{2}\sqrt{4\gamma-\beta}\left(C_0-t\right)\right]\right\}.V(x). \tag{38}$$

Having the values of the functions U_1(σ, x) and U_2(σ, x, t), we obtain the final solution to the problem:

$$U(\sigma,x,t)=\left\{\exp\left(-\varepsilon^2\sigma\right)+\frac{1}{2}\exp\left(-\varepsilon^2\sigma\right)\left\{1+\sqrt{\frac{4\gamma-\beta}{\beta}}Tan\left[\frac{\sqrt{\beta}}{2}\sqrt{4\gamma-\beta}\left(C_0-t\right)\right]\right\}\right\}.V(x). \tag{39}$$

From the boundary condition of the problem (17), it follows $U(0,x,0)=\phi(x)$. Therefore,

$$U(0,x,0)=\left\{\frac{3}{2}+\frac{1}{2}\sqrt{\frac{4\gamma-\beta}{\beta}}Tan\left[\frac{\sqrt{\beta(4\gamma-\beta)}}{2}C_0\right]\right\}V(x)=\phi(x). \tag{40}$$

Integrating the resulting Eq (40) on the interval [0.01, 1], we get:

$$\frac{3}{2}+\frac{1}{2}\sqrt{\frac{4\gamma-\beta}{\beta}}Tan[Z]=\frac{\int_{0.01}^{1}\phi(x)dx}{b}, \tag{41}$$

where

$$Z = \frac{\sqrt{\beta(4\gamma - \beta)}}{2} C_0 \tag{42}$$

Considering the value of the function $V(x)$ from Eqs (23) and (33), we determine the values b and γ of the coefficients:

$$b = \int_{0.01}^{1} V(x)dx = \int_{0.01}^{1} \left[C_1 \int_{0.01}^{x} \frac{e^{\xi}}{\xi} d\xi \right] dx = 4.205 C_1, \quad \gamma = \frac{0.235 f(\sigma,t)}{C_1} \tag{43}$$

With these determined values of the coefficients, we get:

$$Tan[Z] = \frac{1}{\sqrt{0.942 \frac{f(\sigma,t)}{C_1} - \beta}} \left[\frac{0.471\sqrt{\beta} \int_{0.01}^{1} \phi(x)dx}{C_1} - 3\sqrt{\beta} \right]. \tag{44}$$

Equation (44) has real roots if Z = 1. Based on the general solution of the problem, we obtain solutions for particular cases, assuming $\beta = 0.1$, $F(\sigma,t) = 1$, and $\varphi(x) = 1$, and we obtain $C_1 = 0.842$. Substituting these values into Eq (39), we obtain the solution to the problem:

$$U(\sigma,x,t) = \left\{ \exp(-\varepsilon^2\sigma) + \frac{1}{2}\exp(-\varepsilon^2\sigma)[1 + 0.344 Tan(1 - 0.0172t)] \right\} \cdot 0.842 \int_{0.01}^{x} \frac{\exp(y)}{y} dy \tag{45}$$

The resulting equation enables us to obtain a picture of the change in velocities in the entrance transition area. Based on the pattern of velocities, we obtain the formula for the distribution of tangential stresses arising between the fluid layers.

$$\frac{\tau}{\rho R U_0^2} = \left\{ C_1 \left[\exp(-\varepsilon^2\sigma) + \frac{1}{2}\exp(-\varepsilon^2\sigma) \left[1 + \frac{\sqrt{-\beta + 4\gamma}}{\sqrt{\beta}} Tan\left(\frac{\sqrt{\beta(-\beta + 4\gamma)}}{2} (-t + C_0) \right) \right] \right] \exp(x) \right\}^2 \tag{46}$$

Using calculations carried out through computerized experimental research, graphs of instantaneous velocities and tangential stresses arising between fluid layers were plotted, which graphically express the regularities of their change.

3. Results

Graphs of changes in axial velocities and shear stresses along the length of the hydrodynamic entrance region of an axisymmetric pressure flow were created using numerical calculations based on the regularities of changes in the hydrodynamic parameters of an incompressible fluid at the inlet section of an axisymmetric pressure flow. The following geometric parameters $U(0,x,0) = \phi(x) = 1$

were used in calculations. Figures 2 and 4 were plotted based on Eq (45) and Figure 5 was based on Eq (46). Table 1 provides the numerical values of the curves displayed in Figure 2.

Table 1. Numerical values of Figure 2 curves' coordinates are of the function $U_x(\sigma,x,t)$.

x \ σ	0.1	1.0	5	10	15
0.1	3.31	3.02	2.03	1.23	0.75
0.2	4.42	4.04	2.71	1.64	0.995
0.4	5.7	5.21	3.50	2.12	1.28
0.6	6.62	6.05	4.05	2.46	1.49
0.8	7.42	6.78	4.54	2.75	1.67
1.0	8.17	7.47	5.00	3.04	1.84

Graphs showing variations in axial velocities were plotted for various cross-sections in the hydrodynamic entrance region based on the data in Table 1.

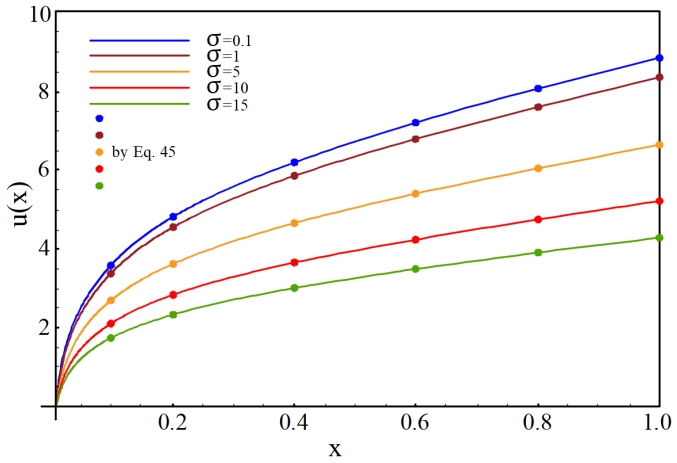

Figure 2. Graphs of changes in the axial velocities $U(\sigma,x,t)$ along the hydrodynamic entrance region of axisymmetric unsteady turbulent flow at $F(\sigma,t)=1$, $\varphi(x)=1$, $\beta=0.1$, $t=10$, $\sigma\to\{0.1,1,5,10,15\}$, and $\varepsilon^2=0.1$.

The resulting graphs indicate regularities in velocity change throughout the entrance region. This makes it possible to evaluate the amount and pattern of velocity change at various points in time, which is crucial for fluid power system entry region design.

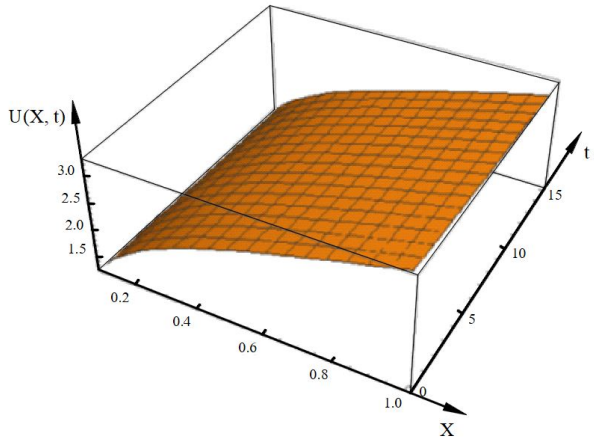

Figure 3. Schematic spatial representation of the change in axial velocity $u[x,t]$ at $\sigma = 10, \{t, 0,15\}, \{x, 0.1,1\}]$.

The 3D view of the time-dependent variation of the axial velocity at a fixed point of the cross-section in the entrance region was plotted. The numerical values of curves shown in Figure 4 are given in Table 2.

Table 2. Numerical values of Figure 4 curves' coordinates are determined by $U_\sigma(\sigma,x,t)$.

x \ σ	0	10	20	30	40	50
0.1	3.48	1.28	0.47	0.17	0.064	0.023
0.3	5.39	1.98	0.73	0.27	0.099	0.036
0.5	6.49	2.39	0.88	0.32	0.12	0.044
0.7	7.38	2.71	1.00	0.37	0.14	0.05
0.9	8.19	3.01	1.11	0.41	0.15	0.055

Graphs showing variations in axial velocities were plotted along the length of the hydrodynamic entrance region based on the data given in Table 2.

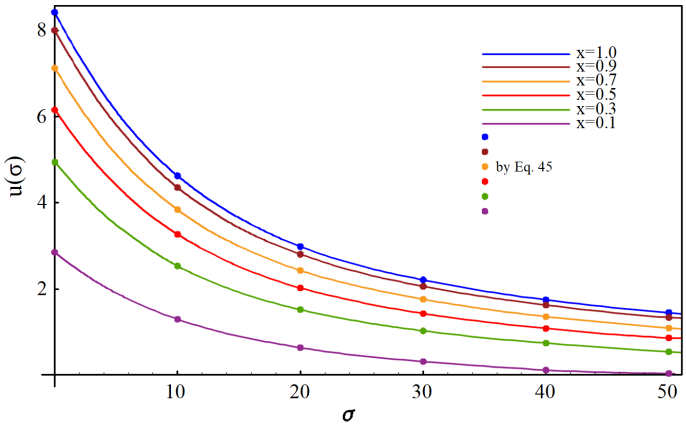

Figure 4. Graphs of changes in axial velocities $U(\sigma,x,t)$ along the length of the hydrodynamic entrance region in the interval $\{\sigma,\ 0;\ 50\}$ at $F(\sigma,t)=1$, $\phi(x)=1$, $\beta=0.1$, $t=10$, $x\to\{0.1,0.3,0.5,0.7,0.9,1\}$, and $\varepsilon^2=0.1$.

Estimating the length of the pipe's stabilized section and designing the entry region to ensure smooth operation were made possible by the obtained graphs of the velocity change along the entrance region. The numerical values of the curves shown in Figure 5 are given in Table 3.

Table 3. Numerical values of Figure 5 curves' coordinates are determined by function $\frac{\tau}{\rho R U_0^2}$.

σ \ x	0,1	0.2	0.4	0.6	0.8	1.0
0.1	12.06	9.88	6.62	4.44	2.97	1.99
1.0	10.78	8.83	5.92	3.96	2.66	1.78
5.0	6.82	5.58	3.74	2.51	1.68	1.13
10.0	4.20	3.44	2.31	1.55	1.04	0.69
15.0	2.85	2.33	1.56	1.05	0.7	0.47

Graphs showing changes in tangential stresses between layers of the fluid at different cross-sections of the hydrodynamic entrance region were plotted based on the data in Table 3.

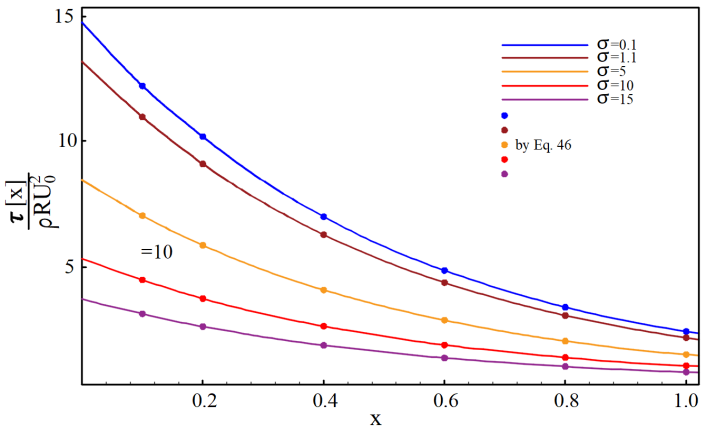

Figure 5. Graphs of changes in tangential stresses $\frac{\tau}{\rho R U_0^2}$ in different sections of the hydrodynamic entrance region of a round pipe at $F(\sigma,t)=1$, $\phi(x)=1$, $\beta=0.1$, $\varepsilon^2=0.1$, $t=10$, $x(0;1)$, and $\sigma \to \{0.1,1.5,10,15\}$.

Estimating the length of the pipe's stabilized section and designing the entry region to ensure smooth operation were made possible by the obtained graphs of the velocity change along the entrance region.

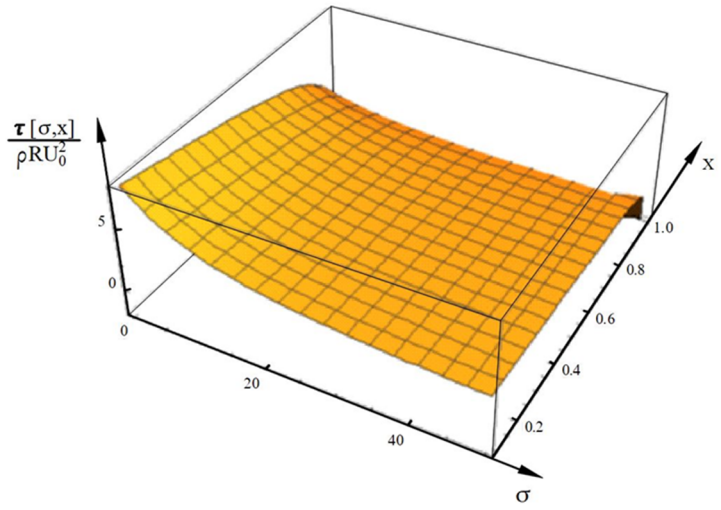

Figure 6. Schematic spatial representation of the change in tangential stresses $\frac{\tau[\sigma,x]}{\rho RU_0^2}$ when $\{\sigma,0,50\}$, $\{x,0.1,1\}$, $F(\sigma,\mathrm{t})=1$, $\phi(x)=1$, $\beta=0.1$, $\varepsilon^2=0.1$, and $t=10$.

The obtained graphs provide an opportunity to gain an idea of the patterns of changes in the hydrodynamic parameters of the flow in the entrance transition area under conditions of unsteady axisymmetric flow. Based on the nature of the revealed patterns, it is necessary to design the transition sections of automatic control systems in such a way that they will ensure smooth flow of current, ensuring precise operation of the equipment.

The formula used to calculate the tangential stresses that develop between liquid layers in turbulent flows was chosen solely to formulate the boundary problem and provide analytical solutions. We believe that this research is valuable from a theoretical and applied points of view. The problem under discussion is one of the classical problems of applied hydromechanics. Therefore, its solution can contribute to the correct design of the hydrodynamic entrance region of automatic control hydraulic equipment. Further studies of the mentioned problem can be carried out, considering the refined patterns of the kinematic coefficient's variations of fluid viscosity. However, the introduction of complex models of the kinematic viscosity coefficient leads to a more complex boundary value problem, the integration of which can lead to insurmountable difficulties.

Almost no research has been done on this practical issue. The mechanisms of developed tangential stresses in turbulent flows were the subject of most research. We have studied a related issue for stationary flow and published a paper [32]. The outcomes of the aforementioned work were compared. To do this, graphs of the velocity change under stationary flow were plotted for the regions of $\sigma\rightarrow\{1,6,10\}$.

The below equation of stationary flow

$$\mathrm{U}(\sigma,x)=\{(e^{-0.1\sigma}+1.14184\mathrm{Tanh}[0.114184\sigma-1])(1.80583\int_{0.01}^{x}\frac{e^{y}}{y}dy)\} \tag{47}$$

was used to plot coordinates of the graph of velocity change in the sections $\sigma\rightarrow\{1,6,10\}$ (Table 4).

A graph of the change in velocity under stationary flow was plotted using the coordinates provided in Table 4 (Figure 7).

Table 4. Coordinates of the velocity change graph under steady flow conditions.

σ \ x	0.1	0.2	0.4	0.6	0.8	1.0
1.0	0.41	0.55	0.71	0.82	0.92	1.01
6.0	0.87	1.17	1.49	1.74	1.94	2.14
10	2.29	3.05	3.94	4.57	5.12	5.65

In the case of unsteady flow, the patterns of change of the hydrodynamic parameters of the flow over time tend to the patterns corresponding to the conditions of stationary flow under the same conditions. Therefore, the comparison of the parameters should be performed when t→∞ in the case of the unsteady flow equation, which is derived from Eq (45) by setting t = ∞.

$$U(\sigma, x, \mathrm{t} = \infty) = \{1.22996 e^{-0.1\sigma}(0.842 \int_{0.01}^{x} \frac{e^{y}}{y} dy)\} \tag{48}$$

Equation (48) determines the coordinates of the velocity change graph for the sections σ→{1,6,10} (Table 5).

Table 5. Coordinates of the velocity change graph in case of unsteady flow.

σ \ x	0.1	0.2	0.4	0.6	0.8	1.0
1.0	0.91	1.22	1.57	1.82	2.04	2.25
6.0	1.36	1.82	2.34	2.72	3.05	3.36
10	2.24	3.00	3.86	4.49	5.03	5.54

A graph of the change in velocity in case of stationary flow was plotted using the coordinates provided in Table 5 (Figure 7).

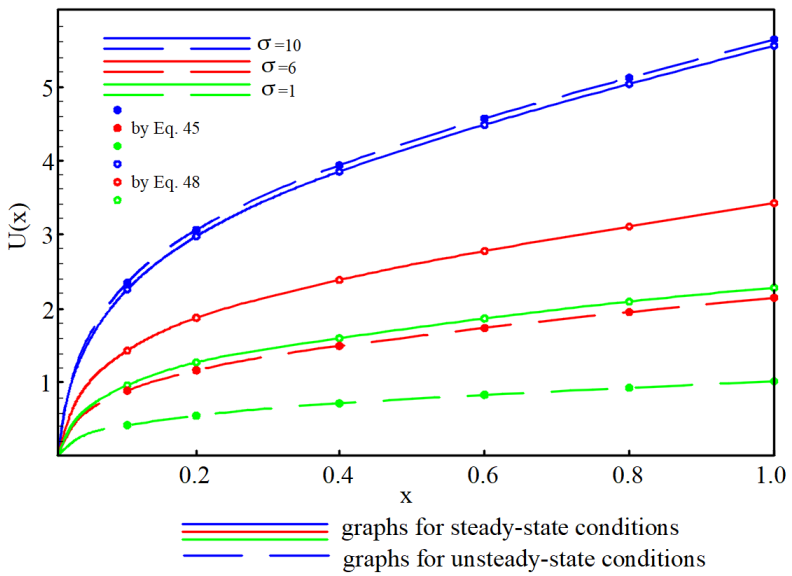

Figure 7. Graphs of velocity in the hydrodynamic entrance region σ→{1,6,10}.

From the comparison of the obtained graphs, we conclude that deviations are observed in the sections close to the entrance ($\sigma \to 1.6$). At a certain distance from the entrance, the mentioned deviations disappear, and the graphs coincide ($\sigma \to 10$). The comparisons made prove the reliability of the conducted research.

4. Discussion of the findings on the development of a viscous fluid unsteady flow at the round pipe inlet section

A boundary value problem was developed based on Eqs (1)–(4) that were obtained by a linear approximation of the system of differential equations of unsteady flow of a viscous fluid in a dense medium. Prandtl's formula was used to determine the tangential stresses that developed between the fluid layers (11). The boundary conditions of the problem were defined as (16) and (17). A method was developed for the integration of the formulated boundary problem, as a result of which the dynamics of the change in axial velocities (45) and tangential stresses (46) developing between the fluid layers were determined. Axial velocity and tangential stress variations' graphs were plotted for different points of the effective cross-section on the basis of performed computer-aided experimental studies (Figures 2–6).

Due to the deformation of the diagrams and the impact of the pressure gradient, the velocity diagrams' shapes in each fixed segment of the input region vary over time (Figure 2). The flow of viscous fluid is unstable when there is unsteady flow in the hydrodynamic entrance region. The pressure gradient is what causes the velocity profile to change outside the hydrodynamic inlet area. Turbulent shear forces were taken into consideration when examining the evolution of the viscous fluid flow in a round pipe's entrance area. The precision of the integration findings is acceptable to engineering practice. Moreover, our findings may be used to the design of hydraulic systems' input units for a variety of machinery and mechanisms, guaranteeing more dependable and seamless functioning. Additionally, to identify the patterns of change of hydrodynamic parameters of unstable turbulent flow in the hydrodynamic entrance region of a round pipe, if the change in the kinematic viscosity coefficient is considered, a thorough analysis of the problem is required due to its significance. We were able to ascertain the length of the first part by analyzing the outcomes of numerical computations and the resulting graphs. The axial velocity variation in the transition section at $x = 1$ should not be greater than 1% of the stable section's varying velocity. Further studies of the mentioned problem can be carried out, taking into account the refined patterns of the kinematic coefficient's variations of fluid viscosity. However, the introduction of complex models of the kinematic viscosity coefficient leads to a more complex boundary value problem, the integration of which can lead to insurmountable difficulties.

The use of more intricate models of the fluid flow regime at the hydrodynamic entrance region and the related consideration of the shear stress between the fluid layers would further improve the suggested study. Integration presents unsolvable mathematical challenges when considering intricate shear stress models. The suggested issue is one of the traditional problems in classical hydromechanics, and its solutions produce a number of conclusions that are helpful for engineering applications and scientific study.

5. Conclusions

1) The regularity of changes in the hydrodynamic characteristics of the flow under general boundary conditions may be obtained using the suggested universal technique to calculate the rearrangement of velocities in the transition section of the round pipe inlet. The estimated equations of flow of a viscous fluid serve as the foundation for the problem's mathematical model, which uses the Prandtl formula to calculate the viscous forces. The patterns of axial velocity variations in the inlet transition area were found for broad boundary conditions by formulating a boundary value problem and developing an integration technique.

2) In order to determine the process of deformation of the velocity field in the transition section of the cylindrical pipe inlet, it is crucial to calculate changes in the hydrodynamic parameters of the flow and make generalizations. Thus, computer experimental studies were conducted based on the obtained analytical solutions, and distribution profiles of axial velocities change and tangential stresses were constructed. Furthermore, correctly building the corresponding units of hydromechanical equipment was made possible by identifying regularities of velocity field changes in the transition section and the graphs built on their basis.

Use of AI tools declaration

The authors declare they have not used Artificial Intelligence (AI) tools in the creation of this article.

Conflict of interest

The authors declare there are no conflicts of interest.

References

1. L.Y. Ainola, Ruustal, Flow development at the inlet section of a round pipe during accelerating fluid movement, in *Proceedings of the Tallinn Polytechnic Institute*, Tallinn, (1985), 95–107.
2. A. Reci, A. Sederman, L. Gladden, Experimental evidence of velocity profile inversion in developing laminar flow using magnetic resonance velocimetry, *J. Fluid Mech.*, **851** (2018), 545–557. https://doi.org/10.1017/jfm.2018.512
3. K. Urbanowicz, M. Firkowski, A. Bergant, Comparing analytical solutions for unsteady laminar pipe flow, in *Proceedings of the 13th International Conference on Pressure Surges*, Bordeaux, France, (2018), 14–16.
4. T. Wiens, E. Etminan, An analytical solution for unsteady laminar flow in tubes with a tapered wall thickness, *Fluids*, **6** (2021), 170. https://doi.org/10.3390/fluids6050170
5. A. E. Vardy, M. B. Brown, Laminar pipe flow with time-dependent viscosity, *J. Hydroinf.*, **13** (2011), 729–740. https://doi.org/10.2166/hydro.2010.073
6. A. Sarukhanyan, Y. Vartanyan, P. Baljyan, G. Vermishyan, Pattern identification of the non-stationary laminar flow of a viscous fluid in the round pipe inlet section, *East.-Eur. J. Enterp. Technol.*, **2** (2023), 33–42. https://doi.org/10.15587/1729-4061.2023.278001

7. A. Sarukhanyan, A. Vartanyan, G. Vermishyan, V. Tokmajyan, The study of hydrodynamic processes occurring on transition of sudden expanding of hydraulic section of plane-parallel full pipe flow, *TEM J.*, **9** (2020), 1494–1501. https://doi.org/10.18421/tem94-23
8. A. Sarukhanyan, G. Vermishyan, H. Kelejyan, Plane-parallel laminar flow of viscous fluid in the transition zone of the inlet section, *J. Archit. Eng. Res.*, **4** (2023), 75–85. https://doi.org/10.54338/27382656-2023.4-008
9. A. Kannaiyan, S. Natarajan, B. R. Vinoth, Stability of a laminar pipe flow subjected to a step-like increase in the flow rate, *Phys. Fluids*, **34** (2022), 064102. https://doi.org/10.1063/5.0090337
10. B. Lebon, J. Peixinho, S. Ishizaka, Y. Tasaka, Subcritical transition to turbulence in a sudden circular pipe expansion, *J. Fluid Mech.*, **849** (2018), 340–354. https://doi.org/10.1017/jfm.2018.421
11. G. Shajari, M. Abbasi, M. Jamei, Entrance length of oscillatory flows in parallel plate microchannels, *Proc. Inst. Mech. Eng., Part C: J. Mech.*, **235** (2021), 3833–3843. https://doi.org/10.1177/0954406220968125
12. M. K. Wong, L. C. Sheng, C. S. Nor Azwadi, G. A. Hashim, Numerical study of turbulent flow in pipe with sudden expansion, *J. Adv. Res. Fluid Mech. Thermal Sci.*, **6** (2015), 34–48.
13. J. Kühnen, B. Song, D. Scarselli, N. B. Budanur, M. Riedl, A. P. Willis, et al., Destabilizing turbulence in pipe flow, *Nat. Phys*., **4** (2018), 386–390. https://doi.org/10.1038/s41567-017-0018-3
14. I. Daprà, G. Scarpi, Unsteady flow of fluids with arbitrarily time-dependent rheological behavior, *J. Fluids Eng.*, **139** (2017), 051202. https://doi.org/10.1115/1.4035637
15. R. Gerardo, J. P. Robert, J. O. Paulo, Bifurcation phenomena in viscoelastic flows through a symmetric 1:4 expansion, *J. Non-Newtonian Fluid Mech.*, **141** (2007), 1–17. https://doi.org/10.1016/j.jnnfm.2006.08.008.
16. E. Gücüyen, R. T. Erdem, Ü. Gökkuş, Numerical modelling of sudden contraction in pipe flow, *Sigma J. Eng. Nat. Sci.*, **37** (2019), 903–916.
17. T. Mullin, J. R. T. Seddon, M. D. Mantle, A. J. Sederman, Bifurcation phenomena in the flow through a sudden expansion in a circular pipe, *Phys. Fluids*, **21** (2009), 014110. https://doi.org/10.1063/1.3065482
18. H. Takumi, R. Zvi, Viscous flow in a slightly asymmetric channel with a sudden expansion, Physics of Fluids, **12** (2000), 2257–2267. https://doi.org/10.1063/1.1287610
19. V. Fester, B. Mbiya, P. Slatter, Energy losses of non-Newtonian fluids in sudden pipe contractions, *Chem. Eng. J.*, **145** (2008), 57–63. https://doi.org/10.1016/j.cej.2008.03.003
20. X. Chen, F. Hussain, Z. S. She, Quantifying wall turbulence via a symmetry approach. Part 2. Reynolds stresses, *J. Fluid Mech.*, **850** (2018), 401–438. https://doi.org/10.1017/jfm.2018.405
21. R. Baidya, J. Philip, N. Hutchins, J. P. Monty, I. Marusic, Distance-from-the-wall scaling of turbulent flows in wall-bounded flows, *Phys. Fluids*, **29** (2017), 020712. https://doi.org/10.1063/1.4974354
22. P. Luchini, Universality of the turbulent velocity profile, *Phys. Rev. Lett.*, **118** (2017), 224501. https://doi.org/10.1103/PhysRevLett.118.224501
23. D. Lunia, R. Mundhra, S. Majumder, Numerical investigation of turbulent flow in a sudden expansion, in *Proceedings of the 25thNational and 3rdInternationalISHMT-ASTFE Heat and Mass Transfer Conference (IHMTC-2019)*, 2019.
24. B. H. Sun, Closed form solution of plane-parallel turbulent flow along an unbounded plane surface, *Preprints*, 2022. https://doi.org/10.20944/preprints202111.0008.v4

25. L. Liu, S. N. Gadde, R. J. A. M. Stevens, Universal wind profile for conventionally neutral atmospheric boundary layers, *Phys. Rev. Lett.*, **126** (2021), 104502. https://doi.org/10.1103/PhysRevLett.126.104502
26. T. I. Józsa, Analytical solutions of incompressible laminar channel and pipe flows driven by in-plane wall oscillations, *Phys. Fluids*, **31** (2019), 083605. https://doi.org/10.1063/1.5104356
27. M. Kharghani, M. P. Fard, Turbulence structures in accelerated flow over a plane plate with non-zero pressure gradient, *J. Appl. Fluid Mech.*, **15** (2022), 311–324. https://doi.org/10.47176/jafm.15.02.32337
28. Y. V. Chovnyuk, V. T. Kravchuk, A. S. Moskvitina, I. O. Peftevaa, Numerical simulation of the non-stationary flow of a viscous incompressible liquid in flat channels of arbitrarily shaped heat exchangers, *Vent., Light. Heat Gas Supply*, **34** (2020), 41–55. https://doi.org/10.32347/2409-2606.2020.34.41-55
29. H. Schlichting, K. Gersten, *Boundary-Layer Theory*, Springer, Berlin, Heidelberg, 2016.
30. S. M. Targ, *Main Problems of the Theory of Lamiar Flows*, Moscow, Gostekhizdat, (1951), 420.
31. A. N. Tikhonov, A. G. Samarski, *Equations of Mathematical Physics*, Moscow, Nauka, (1999), 799.
32. A. Sarukhanyan, G. Vermishyan, H. Kelejyan, V. Baljyan, Study of viscous fluid turbulent stationary flow in the transition section of the inlet section of a circular cylindrical pipe, *Int. J. Innovative Res. Sci. Stud.*, **8** (2025), 86–96. https://doi.org/10.53894/ijirss.v8i10.10744

AIMS Press

©2026 the Author(s), licensee AIMS Press. This is an open access article distributed under the terms of the Creative Commons Attribution License (https://creativecommons.org/licenses/by/4.0)